Heterogeneously Catalyzed Selective Acceptorless Dehydrogenative Aromatization to Primary Anilines from Ammonia via Concerted Catalysis and Adsorption Control

Hui Li, Takafumi Yatabe,* Satoshi Takayama, and Kazuya Yamaguchi*

Cite This: *JACS Au* 2023, 3, 1376−1384

Read Online

ACCESS | Metrics & More | Article Recommendations | SI Supporting Information

ABSTRACT: Although catalytic dehydrogenative aromatization from cyclohexanones and NH_3 is an attractive synthetic method for primary anilines, using a hydrogen acceptor was indispensable to achieve satisfactory levels of selectivity in liquid-phase organic synthetic systems without photoirradiation. In this study, we developed a highly selective synthesis of primary anilines from cyclohexanones and NH_3 via efficient acceptorless dehydrogenative aromatization heterogeneously catalyzed by an $Mg(OH)_2$-supported Pd nanoparticle catalyst in which $Mg(OH)_2$ species are also deposited on the Pd surface. The basic sites of the $Mg(OH)_2$ support effectively accelerate the acceptorless dehydrogenative aromatization via concerted catalysis, suppressing the formation of secondary amine byproducts. In addition, the deposition of $Mg(OH)_2$ species inhibits the adsorption of cyclohexanones on the Pd nanoparticles to suppress phenol formation, achieving the desired primary anilines with high selectivity.

KEYWORDS: *acceptorless dehydrogenative aromatization, adsorption control, ammonia, concerted catalysis, primary anilines*
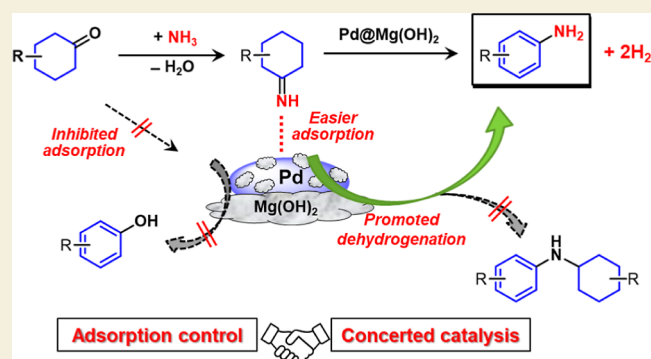
INTRODUCTION

Primary anilines are important basic chemicals widely utilized in diverse fields such as organic synthesis, pharmaceuticals, agrochemicals, dyes, electronic materials, polymers, and other industrial chemicals.[1] These relevant compounds are conventionally prepared via classical nitration of arenes followed by reduction of nitrobenzenes;[2] however, this multistep process requires a large amount of acids and cannot directly utilize NH_3 as the nitrogen source, which is highly convenient because NH_3 is industrially produced from N_2 and H_2 in large quantities. Up to now, various methods have been developed for the synthesis of primary anilines using NH_3, for example, transition metal-catalyzed cross-coupling reactions between aryl halides or arylboronic acids and NH_3 (Figure 1a),[3] phenol conversion to anilines using NH_3 via a dearomatization/rearomatization sequence (Figure 1b),[4,5] and C–H amination of arenes with NH_3.[6] Unfortunately, these approaches require prefunctionalization, (super)stoichiometric amounts of bases, and/or addition of reductants, and the substitution patterns of arene substrates are limited to *ortho/meta/para* orientation.

In this context, the catalytic dehydrogenative aromatization of nonaromatic compounds like cyclohexanones, which can be regioselectively functionalized without the limitation of *ortho/meta/para* orientation, offers an environmentally friendly tool to access various aromatic compounds without using leaving or directing groups.[7−10] In 2019, we developed a selective synthesis of primary anilines via dehydrogenative aromatization from cyclohexanones using NH_3 as the nitrogen source in the presence of a hydroxyapatite (HAP)-supported Pd nanoparticle catalyst (Pd/HAP) (Figure 1c).[8a] However, this method requires a stoichiometric amount of styrene as the hydrogen acceptor to avoid undesirable conversion of primary anilines to secondary anilines, which occurs preferentially via reductive *N*-alkylation with cyclohexanones or cyclohexanimine intermediates (Figure 1c).[8] Although we also reported new hydrogen acceptor-free synthesis methods for primary anilines from cyclohexanones, using hydroxylamine or hydrazine as the nitrogen source was indispensable to achieve high efficiency and selectivity.[8b,c] Recently, a homogeneously catalyzed photoredox acceptorless dehydrogenative amination from cyclohexanones and NH_3 to access primary anilines was developed.[9] Despite these impressive achievements, the selective synthesis of primary anilines from NH_3 via thermally catalyzed acceptorless dehydrogenative aromatization remains
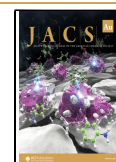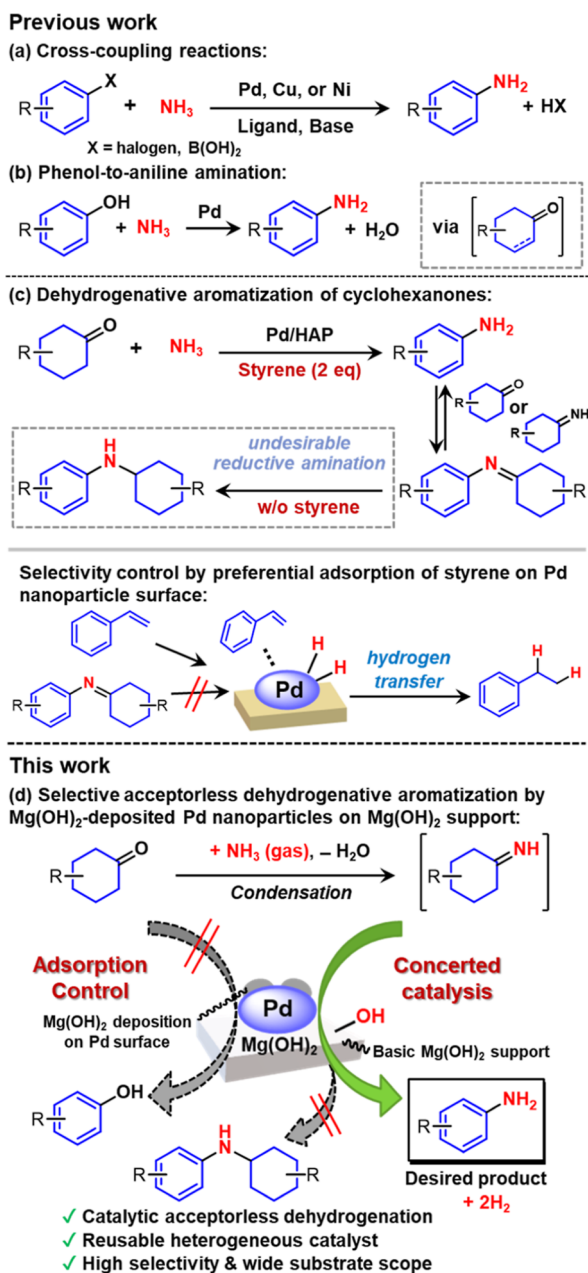
Figure 1. Synthesis of primary anilines using NH$_3$ as the nitrogen source.

as an important challenge mainly because of difficulties in selectivity control.[11]

In recent years, our group has focused on the design of Pd-based heterogeneous catalysts for efficient dehydrogenative aromatization reactions.[8,10] Especially, concerted catalysis between supported Pd nanoparticles and neighboring basic sites of the support, e.g., a layered double hydroxide (LDH), was revealed to be important to achieve an efficient dehydrogenative aromatization of cyclohexanones (cyclohexanols) and cyclohexanone oximes to phenols and primary anilines, respectively.[8b,10a,b] Considering that reductive *N*-alkylation between primary anilines and cyclohexanimine intermediates to secondary anilines is a common side reaction in the acceptorless dehydrogenative aromatization to primary anilines,[8b,c] we envisioned that using basic supports could promote the desired dehydrogenation of cyclohexanimine

intermediates to efficiently afford primary anilines, inhibiting the formation of secondary amines. However, concerted catalysis using basic supports could result in the formation of phenols via direct dehydrogenation of cyclohexanones.[10a,b] Thus, phenol formation must be also inhibited to produce primary anilines with high selectivity.

In our previous work, the preferential adsorption of styrene on the Pd nanoparticle surface was the key to inhibit side reactions like hydrogenation of secondary imines to the corresponding secondary amine byproducts, enabling the selective dehydrogenative aromatization to primary anilines (Figure 1c).[8a] In addition, we found that phenol formation was also suppressed to a considerable extent due to styrene adsorption when analyzing the phenol synthesis via dehydrogenative aromatization using an LDH-supported Pd nanoparticle catalyst (Pd/LDH, LDH = Mg$_6$Al$_2$(OH)$_{16}$(CO$_3$)· 4H$_2$O) in the absence or presence of styrene (Scheme S1). Therefore, if the Pd nanoparticle surface was suitably modified by something other than hydrogen acceptors, phenol formation from cyclohexanones would be inhibited via adsorption control even under the acceptorless conditions. Given the aforementioned concerted catalysis with basic supports and the general deactivation by coverage of the catalyst surface,[12] basic supports-immobilized Pd nanoparticle catalysts with the surface modification by the basic supports will be promising for the efficient selective acceptorless dehydrogenative aromatization to primary anilines.

Herein, we describe the successful development of a selective acceptorless dehydrogenative aromatization to primary anilines from readily available cyclohexanones using NH$_3$ as the nitrogen source and an Mg(OH)$_2$-supported Pd nanoparticle catalyst in which Mg(OH)$_2$ species are deposited on the Pd surface (Pd@Mg(OH)$_2$) (Figure 1d). By combining the concerted catalysis with the basic support and the adsorption control via Pd nanoparticle surface modification, high selectivity to primary anilines was achieved. The catalyst was confirmed to be heterogeneous and reusable several times without severe loss of its catalytic performance. Also, a wide substrate scope was demonstrated, selectively affording structurally diverse primary anilines in high yields via acceptorless dehydrogenative aromatization.

■ RESULTS AND DISCUSSION

Pd@Mg(OH)$_2$ was prepared via deposition–precipitation of Pd species in water using MgO as the support, which was converted into Mg(OH)$_2$ during this process, followed by NaBH$_4$ reduction (Figure S1a) (Pd: 2.8 wt % determined by an inductively coupled plasma atomic emission spectroscopy (ICP-AES)). We also prepared an Mg(OH)$_2$-supported Pd nanoparticle catalyst without the deposition of Mg(OH)$_2$ species on the Pd surface (Pd/Mg(OH)$_2$) by supporting Pd species on Mg(OH)$_2$ which is produced in advance via the reaction of MgO with water and reducing the Pd species using NaBH$_4$ (Figure S1b) (Pd: 2.8 wt % determined by ICP-AES). The presence of Mg(OH)$_2$ in Pd@Mg(OH)$_2$ and Pd/Mg(OH)$_2$ was confirmed via X-ray diffraction (XRD), which also revealed the absence of Pd species in the XRD patterns (Figure 2a). The X-ray photoelectron spectroscopy (XPS) results of the freshly prepared Pd@Mg(OH)$_2$ and Pd/Mg(OH)$_2$ catalysts were almost the same around the Pd 3d region, revealing their similar electronic states and Pd^0/Pd^{2+} ratios (~77/23) (Figure 2b). According to transmission electron microscopy (TEM) observations, Pd species having
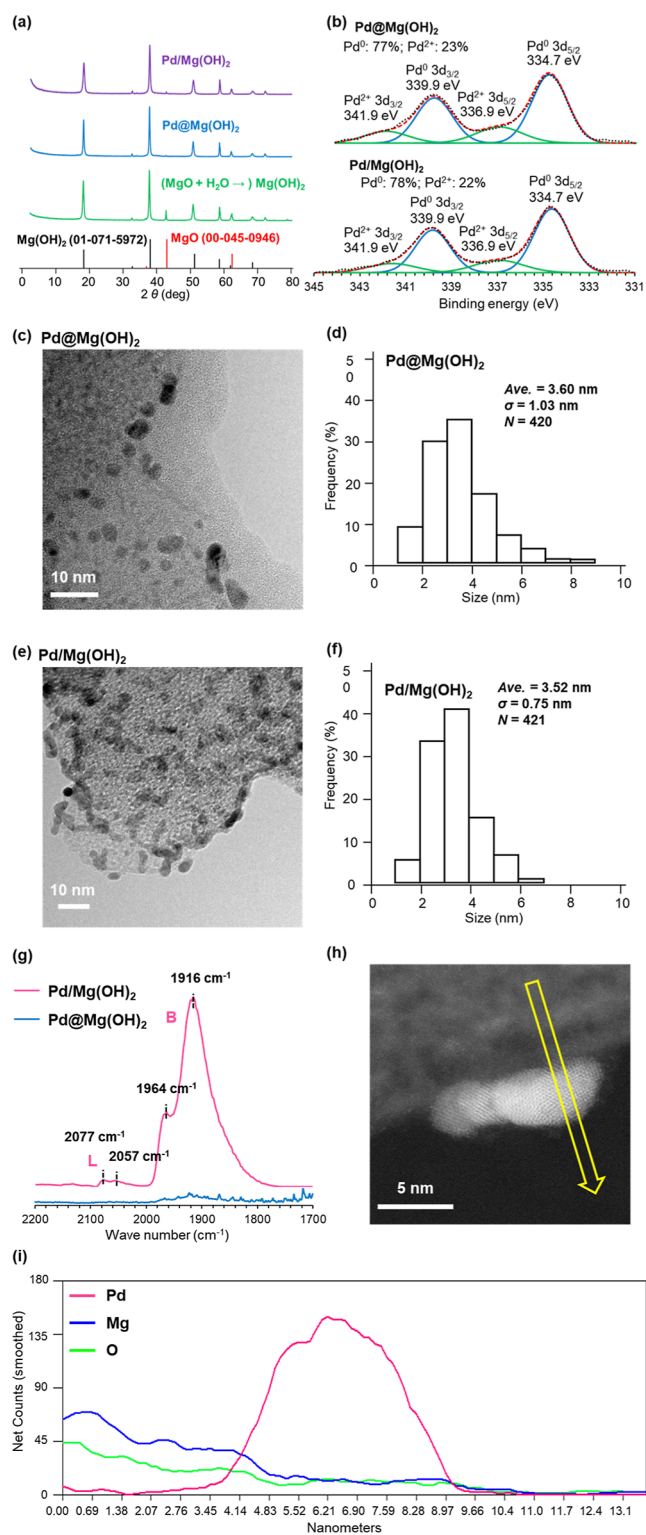
Figure 2. Characterization of Pd@Mg(OH)$_2$ and Pd/Mg(OH)$_2$: (a) XRD patterns of Pd/Mg(OH)$_2$ (purple), Pd@Mg(OH)$_2$ (blue), and Mg(OH)$_2$ (green); (b) XPS spectra of Pd@Mg(OH)$_2$ and Pd/Mg(OH)$_2$; black dot line: data points; blue and green solid lines: deconvoluted signals; red dash line: sum of the deconvoluted signals; (c−f) TEM images and Pd nanoparticle distributions of Pd@Mg(OH)$_2$ and Pd/Mg(OH)$_2$; (g) DRIFTS of CO chemisorption on Pd@Mg(OH)$_2$ (blue) and Pd/Mg(OH)$_2$ (pink); (h) HAADF-STEM image of Pd@Mg(OH)$_2$ and (i) the corresponding EDS line profile across the particle at the position indicated by the yellow arrow.
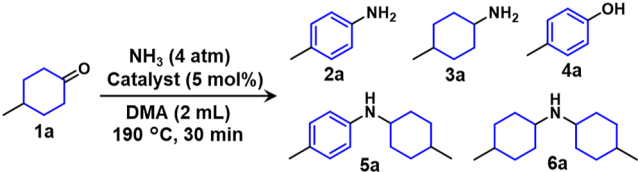
an average size of ∼3.6 nm were dispersedly supported on Mg(OH)$_2$ in both Pd@Mg(OH)$_2$ and Pd/Mg(OH)$_2$ (Figure 2c−f). Moreover, the strength and number of basic sites of the two catalysts were found to be similar by performing Knoevenagel condensation reactions using active methylene substrates with different pK_a (Table S1), considering the difference of the corresponding Brunauer−Emmett−Teller (BET) surface areas (Pd@Mg(OH)$_2$: 21 m^2/g, Pd/Mg(OH)$_2$: 51 m^2/g). Taken together, these results revealed that Pd@Mg(OH)$_2$ and Pd/Mg(OH)$_2$ exhibited similar support structures, Pd oxidation states, Pd electronic states, Pd nanoparticle sizes, and basicity; however, the color of Pd@Mg(OH)$_2$ was shallow gray, whereas that of Pd/Mg(OH)$_2$ was deep gray-black (Figure S1). In addition, both catalysts were subjected to diffuse reflectance infrared Fourier transform spectroscopy (DRIFTS) analysis to evaluate the CO chemisorption on the Pd nanoparticles. In Figures 2g and S2, the spectra after CO adsorption (P_{CO} = ∼200 Torr) followed by 20 min evacuation at room temperature are shown after Kubelka−Munk transformation using the spectra in vacuo before CO adsorption as the backgrounds, indicating only an extremely small CO chemisorption peak in the bridged region in the case of Pd@Mg(OH)$_2$ and large peaks in both linear and bridged regions for Pd/Mg(OH)$_2$ (Figure 2g). These results suggested that CO can be easily adsorbed on Pd/Mg(OH)$_2$, whereas the CO adsorption was suppressed on Pd@Mg(OH)$_2$.

Moreover, when these catalysts were used for the disproportionation reaction of 2-cyclohexen-1-one to cyclohexanone and phenol, which is supposed to occur rapidly on Pd nanoparticles,[10a,b] only Pd/Mg(OH)$_2$ promoted the disproportionation under mild reaction conditions (Scheme S2). These results indicated the presence of some species on the surface of Pd nanoparticles of Pd@Mg(OH)$_2$, which would account for the different reactivity of both catalysts. To further clarify the surface structure of Pd@Mg(OH)$_2$, high-angle annular dark field-scanning TEM (HAADF-STEM) was conducted on Pd@Mg(OH)$_2$ and Pd/Mg(OH)$_2$ (Figures 2h, S3, and S4), which seemed to suggest the presence of deposited compounds on the Pd nanoparticles of Pd@Mg(OH)$_2$. Then, elemental mappings were measured using STEM-energy dispersive X-ray spectroscopy (EDS) of Pd@Mg(OH)$_2$ (Figure S5) to obtain an EDS line profile (Figure 2h,i), clearly revealing the presence of an Mg(OH)$_2$ support region without Pd species (∼0−3.5 nm) and a Pd nanoparticle region with Mg and O species (∼3.5−9.0 nm) whose counts are smaller than those of the Mg(OH)$_2$ support region, which strongly suggested that Mg(OH)$_2$ species were deposited on the Pd nanoparticles of Pd@Mg(OH)$_2$. In contrast, STEM−EDS mappings and an EDS line profile of Pd/Mg(OH)$_2$ indicated almost no count of Mg and O species in the Pd nanoparticle region (Figures S6 and S7), which revealed the absence of Mg(OH)$_2$ species on the surface of Pd nanoparticles of Pd/Mg(OH)$_2$. Overall, these results confirmed the successful preparation of Mg(OH)$_2$-supported Pd nanoparticle catalysts with or without Mg(OH)$_2$ species deposited on the Pd surface, which possessed almost the same support structures, oxidation states and electronic states of Pd species, Pd nanoparticle sizes, and basicity.

After optimizing several conditions (Tables S2−S7), the effect of using different supported Pd nanoparticle catalysts (Pd/Support) and Pd@Mg(OH)$_2$ (the respective loading amounts of Pd catalysts determined by ICP-AES are

summarized in Table S8) on the acceptorless dehydrogenative aromatization from 4-methylcyclohexanone (**1a**) to the corresponding primary aniline (**2a**) was investigated in *N,N*-dimethylacetamide (DMA) solvent at 190 °C for 30 min under 4 atm of NH$_3$ (Table 1). Among the examined catalysts, Pd@

Table 1. Effect of Supported Pd Catalysts on the Acceptorless Dehydrogenative Aromatization from 1a and NH$_3$ to 2a[a]

entry	catalyst	conv. (%)	yield (%)				
			2a	**3a**	**4a**	**5a**	**6a**
1[b]	Pd@Mg(OH)$_2$	96	71	3	3	<1	<1
2[c]	Pd/Mg(OH)$_2$	99	63	5	13	<1	<1
3	Pd/LDH	>99	41	10	26	1	1
4	Pd/HAP	>99	58	16	1	10	<1
5	Pd/CeO$_2$	98	60	9	11	5	1
6[d]	Pd/C	>99	54	19	<1	11	<1
7	Pd/Al$_2$O$_3$	>99	37	12	1	10	4
8	Pd/ZrO$_2$	>99	23	11	<1	6	3
9	Pd/TiO$_2$	>99	25	7	<1	10	8
10[e]	Mg(OH)$_2$	87	<1	<1	<1	<1	<1
11[b]	Pd@Mg(OH)$_2$	>99	56	24	<1	6	1
12[f]	Pd/Mg(OH)$_2$	>99	53	26	<1	7	1
13[g]	Pd/HAP + Mg(OH)$_2$	>99	60	15	1	7	<1

[a]Reaction conditions: **1a** (0.3 mmol), NH$_3$ (4 atm), catalyst (Pd: 5 mol %), solvent (DMA: 2 mL), 190 °C, 30 min. All reactions were conducted in a 40 mL pressure tube. All conversions and yields were determined via GC analysis using *n*-hexadecane as an internal standard. DMA = *N,N*-dimethylacetamide. LDH = layered double hydroxide (Mg$_6$Al$_2$(OH)$_{16}$(CO$_3$)·4H$_2$O). HAP = hydroxyapatite. [b]Average values of two runs. [c]Average values of three runs. [d]Pd/C: 51% water was contained in the catalyst. [e]Mg(OH)$_2$ (60 mg), 1 h. [f]Benzoic acid (0.05 eq. to **1a**) was added to the reaction. [g]Physical mixture of Pd/HAP and Mg(OH)$_2$ (60 mg).

Mg(OH)$_2$ provided the best results, affording **2a** in 71% yield and negligible amounts of 4-methylcyclohexylamine (**3a**), 4-methylphenol (**4a**), or secondary amines (**5a** and **6a**) as byproducts (Table 1, entry 1). In contrast, a considerable amount of **4a** was formed in the presence of Pd/Mg(OH)$_2$ despite having the same Mg(OH)$_2$ support (Table 1, entry 2), which can be attributed to the aforementioned difference in the surface of these two catalysts. Overall, in the presence of basic supports like Mg(OH)$_2$ and LDH (Table S1), the formation of secondary amines was suppressed, whereas phenol was significantly produced except for the case of Pd@Mg(OH)$_2$ (Table 1, entries 2 and 3). In contrast, in the presence of supports having acidic or comparatively weakly basic sites, the formation of secondary amines was inevitable and phenol was hardly produced except for the case of Pd/CeO$_2$ (Table 1, entries 4−9). It should be noted that the electronic states and nanoparticle sizes of the supported Pd nanoparticle catalysts (Table S9) were not correlated with the catalytic performance for the present selective primary aniline synthesis. The Mg(OH)$_2$ support alone did not promote the
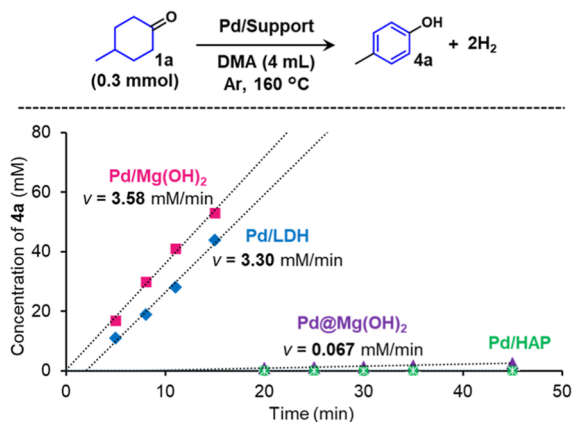
dehydrogenative aromatization to **2a** while the condensation between **1a** and NH$_3$ occurred to produce the corresponding cyclohexanimine, confirming that Pd nanoparticles are the active species in this dehydrogenation reaction (Table 1, entry 10). After the Pd@Mg(OH)$_2$-catalyzed reaction, H$_2$ gas was detected in the gas phase via gas chromatography−mass spectrometry (GC−MS), indicating that this reaction was an acceptorless dehydrogenative process. This catalytic system was also confirmed to be heterogeneous by performing a hot filtration experiment followed by ICP-AES analysis of the filtrate (Pd: below the detection limit) (Figure S8a), and Pd@Mg(OH)$_2$ was demonstrated to be reusable for at least three times without a significant decrease in the **2a** yield (Figure S8b), although TEM observation of Pd@Mg(OH)$_2$ after the third reuse revealed that the average Pd nanoparticle size increased to 5.5 nm during the reusability test (Figure S9; see Supporting Information for details).

To gain more insight into the support effect on the present acceptorless dehydrogenative aromatization to primary anilines, several control experiments were conducted. Adding benzoic acid to the Pd@Mg(OH)$_2$-catalyzed reaction system resulted in a loss of selectivity to aniline **2a** with a decrease in the amount of phenol **4a** and an increase in the production of secondary amine **5a** and cyclohexylamine **3a** (Table 1, entry 11). The same tendency was observed when using Pd/Mg(OH)$_2$ with benzoic acid (Table 1, entry 12). These results suggested that the basic sites of Mg(OH)$_2$ promoted the dehydrogenative aromatization to primary anilines and phenols. In addition, a physical mixture of Pd/HAP and Mg(OH)$_2$ showed almost the same catalytic performance for the present reaction as Pd/HAP (Table 1, entry 13), indicating that the basic sites of Mg(OH)$_2$ near Pd nanoparticles promoted the dehydrogenation reactions via concerted catalysis. According to the proposed reaction pathway (Figure 1d), the concertedly catalyzed dehydrogenative aromatization of cyclohexanimine intermediates, which are formed via the condensation of cyclohexanones and NH$_3$, would inhibit secondary amine formation when using basic supports such as Mg(OH)$_2$. To further clarify the promotion effect of the basic supports, the dehydrogenative aromatization was conducted starting from **3a** via amine oxidation to cyclohexanimine **1a′** under 4 atm of NH$_3$ (Table S10). As a result, the use of basic supports such as LDH and Mg(OH)$_2$ led to a high selectivity to **2a** with almost no formation of secondary amines (Table S10, entries 1−3).[13] In contrast, a weakly basic HAP-supported Pd catalyst resulted in the formation of considerable amounts of **5a** (Table S10, entry 4). Meanwhile, adding benzoic acid to the Pd/Mg(OH)$_2$-catalyzed **3a** dehydrogenation system resulted in the formation of **5a** and a decrease in the **2a** yield (Table S10, entry 5). Using the physical mixture of Pd/HAP and Mg(OH)$_2$ did not increase the **2a** yield, albeit a small decrease in the yield of **5a** was observed (Table S10, entry 6). These results are consistent with those of the dehydrogenative aromatization from **1a** and NH$_3$ (Table 1) and confirmed that basic supports such as Mg(OH)$_2$ promoted the dehydrogenation of cyclohexanimine intermediates to primary anilines via concerted catalysis, which efficiently suppressed the formation of secondary amines.

An investigation of the reaction profile for the Pd@Mg(OH)$_2$-catalyzed dehydrogenative aromatization of **1a** to **2a** under the optimized conditions revealed that a large amount of **2a** and a small amount of **3a** and **4a** were produced at the same time and that the yield of **3a** and **4a** did not

decrease when performing the reaction for 2 h (Figure S10). These results indicate that the main pathway to **2a** is the condensation of **1a** and NH_3 followed by a fast acceptorless dehydrogenative aromatization of intermediate **1a′** to **2a**, which is consistent with the aforementioned concerted catalysis promoting the dehydrogenation of **1a′** and suppressing secondary amine formation. In fact, generally, the dehydrogenative aromatization starting from **3a** afforded **2a** in much lower yields than those obtained in the dehydrogenative aromatization from **1a** and NH_3 (Tables 1 and S10), suggesting that cyclohexylamine oxidation to cyclohexanimine intermediates is comparatively difficult and can be ruled out as the main pathway to primary anilines. Moreover, when the dehydrogenative aromatization of cyclohexanone (**1b**) to aniline (**2b**) was conducted using the Pd@Mg(OH)$_2$-catalyzed system with the addition of **4a**, the dearomatization/rearomatization of **4a** to **1a** did not occur at all (Scheme S3). Thus, the reduction of **4a** is not the reason for the lack of formation of **4a** in the dehydrogenative aromatization to **2a** using Pd@Mg(OH)$_2$.

To investigate why **4a** was hardly produced in the Pd@Mg(OH)$_2$-catalyzed acceptorless dehydrogenative aromatization of **1a** to **2a** despite the presence of the Mg(OH)$_2$ support, the acceptorless dehydrogenative aromatization of **1a** to **4a** was performed without NH_3 using the supported Pd catalysts Pd@Mg(OH)$_2$, Pd/Mg(OH)$_2$, Pd/LDH, and Pd/HAP at 160 °C to measure the respective initial **4a** production rates (Figure 3). As a result, Pd/LDH and Pd/Mg(OH)$_2$ showed high


Figure 3. Reaction profiles showing initial **4a** production rates on the acceptorless dehydrogenative aromatization of **1a** to **4a** catalyzed by different supported Pd catalysts. Reaction conditions: **1a** (0.3 mmol), Ar (1 atm), Pd/Support (Pd: 5 mol %), DMA (4 mL), 160 °C.

catalytic activity to produce **4a**, whereas Pd@Mg(OH)$_2$ and Pd/HAP hardly catalyzed the reaction,[14] which is consistent with the observed tendency in the formation of **4a** in the acceptorless dehydrogenative aromatization of **1a** to **2a** (Table 1, entries 1−4). The basicity of the supports revealed by the Knoevenagel condensation test (Table S1) suggests that the basic sites of Pd/LDH and Pd/Mg(OH)$_2$ promoted effectively the dehydrogenation to **4a** via concerted catalysis, whereas Pd/HAP was inactive because of its weak basicity. However, Pd/Mg(OH)$_2$ and Pd@Mg(OH)$_2$ possess a similar basicity; therefore, this cannot be invoked as the reason behind the lack of reactivity of Pd@Mg(OH)$_2$ toward **4a** formation. Considering the different Pd nanoparticle surface structure of Pd/Mg(OH)$_2$ and Pd@Mg(OH)$_2$, the adsorption of **1a** on the

Pd nanoparticle active sites of Pd@Mg(OH)$_2$ was probably inhibited by the deposition of Mg(OH)$_2$, which suppressed the direct dehydrogenative aromatization of **1a** to **4a**.

Meanwhile, the desired dehydrogenative aromatization of cyclohexanimine **1a′** to **2a** efficiently occurred when using Pd@Mg(OH)$_2$, suggesting the preferential inhibition of cyclohexanone adsorption on Pd nanoparticles. To verify the adsorption control on Pd nanoparticles, hydrogenation reactions of **1a**, **1a′** (formed in situ from **1a** and NH_3), and *N*-(4-methylcyclohexylidene)aniline were performed using H_2 as the reductant over Pd/Mg(OH)$_2$ or Pd@Mg(OH)$_2$ (Figure 4). The hydrogenation of **1a** was found to be more difficult on
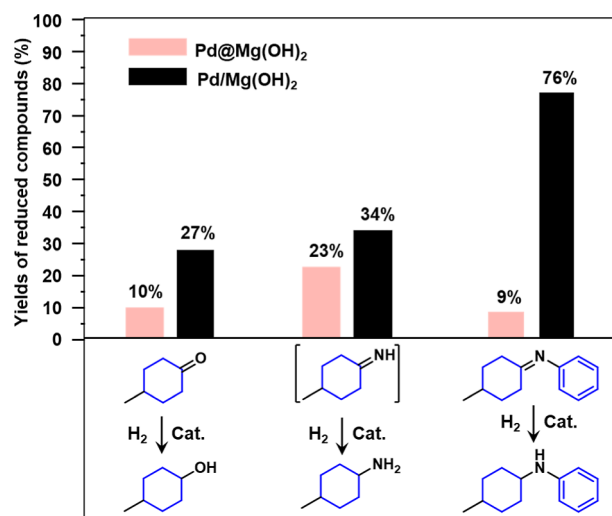

Figure 4. H_2-hydrogenation reactions demonstrating the difference of substrate adsorption on Pd nanoparticles between Pd@Mg(OH)$_2$ and Pd/Mg(OH)$_2$. Reaction conditions (Pd catalyst: 5 mol %, DMA 2 mL): **1a** (0.3 mmol), H_2 (5 atm), 120 °C, 9 h; **1a** (0.3 mmol), NH_3 (4 atm), H_2 (2 atm), 40 °C, 5 h; *N*-(4-methylcyclohexylidene)aniline (0.3 mmol), H_2 (2 atm), r.t., 2 h.

Pd@Mg(OH)$_2$ than on Pd/Mg(OH)$_2$ (10% yield vs 27% yield, respectively), and the hydrogenation of **1a′** was slightly affected by the Mg(OH)$_2$ deposition on Pd nanoparticles (23% yield vs 34% yield, respectively), which indicated that the adsorption of **1a** on the Pd nanoparticles of Pd@Mg(OH)$_2$ is more difficult than that of **1a′**. In this regard, previously reported theoretical studies suggested that substrates with CO groups prefer to adopt planar η^2 adsorption modes such as di-σ adsorption and π adsorption on Pd species,[15] whereas Schauermann and co-workers revealed that a substrate with CN groups exhibits a stable top-mode adsorption on Pd species.[16] Accordingly, the Mg(OH)$_2$ deposition of Pd@Mg(OH)$_2$ could effectively inhibit the planar η^2 adsorption modes of cyclohexanones on Pd nanoparticles while favoring the vertical adsorption mode of cyclohexanimines.[17] In addition, a great difference between Pd/Mg(OH)$_2$ and Pd@Mg(OH)$_2$ was found for the hydrogenation of *N*-(4-methylcyclohexylidene)aniline (Figure 4), suggesting that the secondary imine adsorption was suppressed to a much larger extent on the Pd nanoparticles of Pd@Mg(OH)$_2$.[18] Thus, in the desired dehydrogenative aromatization to primary anilines, Mg(OH)$_2$ deposition on the surface of Pd nanoparticles can also suppress undesired secondary amine formation. All these results confirmed the importance of adsorption control via

modification of the Pd surface for the enhancement of the selectivity to the desired primary anilines.

On the basis of the results presented here and the previous reports on dehydrogenative aromatization,[7,8,10] the following reaction mechanism can be proposed for the selective acceptorless dehydrogenative aromatization of cyclohexanones and NH_3 to primary anilines using Pd@Mg(OH)$_2$ (Figure 5).
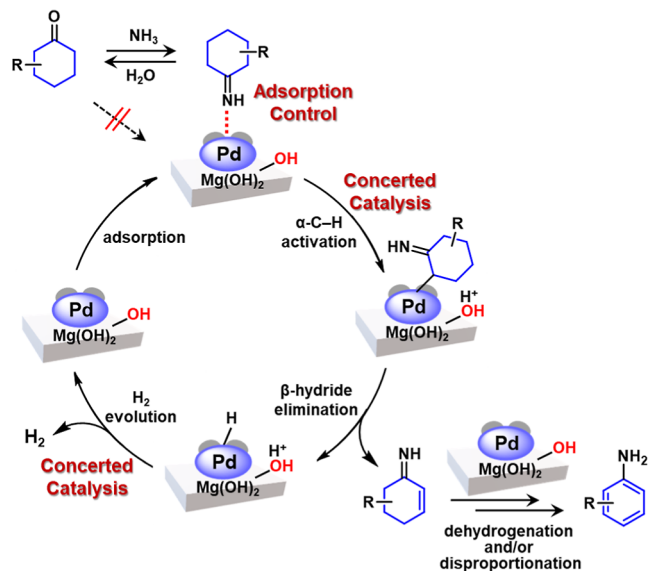
Figure 5. Proposed reaction mechanism for primary aniline synthesis by Pd@Mg(OH)$_2$-catalyzed acceptorless dehydrogenative aromatization via concerted catalysis and adsorption control.

First, the condensation of cyclohexanones and NH_3 forms cyclohexanimine intermediates. After the adsorption of the imines on Pd nanoparticles, α-C−H bond activation occurs via deprotonation/metalation promoted by concerted catalysis between the Pd nanoparticle active sites and the basic sites of Mg(OH)$_2$. Then, α,β-unsaturated imines are formed by β-hydride elimination with formation of Pd−H species, followed by successive dehydrogenation and/or disproportionation on the Pd nanoparticles to produce the desired primary anilines.[19] Finally, the Pd−H species accepts a proton to generate H_2, thereby closing the catalytic cycle. The concerted catalysis between the Pd−H species and the protonated basic sites of Mg(OH)$_2$ can accelerate the H_2 evolution step. The fast conversion of the imine intermediates via concerted catalysis is the key to suppress secondary amine formation. Although the concerted catalysis also promotes the dehydrogenative aromatization of cyclohexanones to phenols, the Mg(OH)$_2$ species deposited on Pd nanoparticles preferentially suppress the adsorption of cyclohexanones on the Pd active sites, improving the selectivity to primary anilines.

Finally, the cyclohexanone scope of the present Pd@Mg(OH)$_2$-catalyzed system for the selective synthesis of primary anilines from NH_3 was investigated under the optimized conditions (Table 2). The substrate conversions and byproduct yields are summarized in Table S11. In some cases (Table 2, entries 11, 18, and 19), to suppress the formation of phenols, the condensation of cyclohexanones and NH_3 was conducted at 50 °C before the dehydrogenation reactions. Cyclohexanone and its alkyl-substituted derivatives were efficiently converted into the corresponding primary anilines (Table 2, entries 1−10). o-Toluidine and 2,5-

dimethylaniline were obtained in good yields despite the relatively slow reaction rates, whereas 2,6-dimethylaniline was produced in a low yield probably because of its large steric hindrance (Table 2, entries 2, 5, and 6). Aryl-substituted cyclohexanones afforded the desired anilines in moderate yields (Table 2, entries 11 and 12). Additionally, cyclohexanones having various functional groups such as trifluoromethyl, ester, alkoxy, amide, and acetal protecting groups were tolerated without obvious decomposition or hydrolysis of the functional groups (Table 2, entries 13−17). 4,4′-Bicyclohexanone was also applicable to this reaction, and 4,4′-diaminobiphenyl and 4-amino-4′-hydroxybiphenyl were obtained as the primary anilines (Table 2, entry 18). In addition to cyclohexanones, 2-cyclohexen-1-one can be applied to this reaction to give the desired primary aniline (Table 2, entry 19).

CONCLUSIONS

In conclusion, we successfully realized the selective synthesis of primary anilines heterogeneously catalyzed by Pd@Mg(OH)$_2$ via an acceptorless dehydrogenative aromatization using NH_3 as the nitrogen source. Various primary anilines were obtained in high yields via concerted catalysis between Pd nanoparticles and the basic sites of the Mg(OH)$_2$ support, enabling the efficient acceptorless dehydrogenative aromatization of cyclohexanimine intermediates to primary anilines while suppressing secondary amine formation. In addition, the modification of the Pd nanoparticle surface via Mg(OH)$_2$ deposition resulted in deactivation of the dehydrogenative aromatization to phenols through preferential suppression of cyclohexanone adsorption on the Pd nanoparticles, enhancing the selectivity to primary anilines even in the presence of the Mg(OH)$_2$ support, which promotes the dehydrogenative aromatization to phenols. Thus, by utilizing a catalyst design unique to heterogeneous catalysis, that is, concerted catalysis between active metal species and supports and the adsorption control on nanoparticles covering the supports, an otherwise difficult selective dehydrogenation reaction is realized. We believe that the findings of this study will pave the way toward novel selective organic transformations by combining various properties specific to heterogeneous catalysts.

EXPERIMENTAL METHODS

Instruments and Reagents

GC analyses were performed on Shimadzu GC-2014 equipped with a flame ionization detector and an InertCap5 capillary column. GC−MS spectra were recorded on Shimadzu GCMS-QP2010 and GCMS-QP2020 equipped with an InertCap5 capillary column at an ionization voltage of 70 eV. Liquid-state nuclear magnetic resonance (NMR) spectra were recorded on JEOL JNM-ECA-500. ^{1}H and ^{13}C NMR spectra were measured at 500.16 and 125.77 Hz, respectively. ^{1}H and ^{13}C NMR chemical shifts were referenced to tetramethylsilane peak (0 ppm) or the solvent peak (^{1}H NMR using CDCl$_3$: δ = 7.26 ppm, DMSO-d_6: δ = 2.50 ppm, ^{13}C NMR using CDCl$_3$: δ = 77.16 ppm, DMSO-d_6: δ = 39.52 ppm). ICP-AES analyses were performed on Shimadzu ICPS-8100. TEM observations were performed on JEOL JEM-2000EX. XRD patterns were measured on Rigaku SmartLab (Cu Kα, 45 kV, 200 mA). XPS results were obtained on Ulvac-Phi PHI5000 VersaProbe. The binding energies were calibrated by using the C 1s signal at 284.8 eV. HAADF-STEM observations were performed on JEM-ARM200F Thermal FE. DRIFTS was performed using the FT/IR-6700 spectrometer (JASCO). MgO (137-10831, 0.05μm, 99.9%, FUJIFILM Wako Pure Chemical), HAP (BET surface area: 11 m^2 g^{-1}, 011-14882, FUJIFILM Wako Pure

Table 2. Substrate scope[a]

Entry	substrate	Product	Entry	substrate	Product	Entry	substrate	Product
1[b]		81%	8[e]		88% (79%)	14		83% (63%)
2[c]		77%	9[e]		72% (60%)	15		67% (55%)
3		70%	10[f]		86% (80%)	16[i]		58% (57%)
4		77% (76%)	11[g]		40% (37%)	17[e]		87% (63%)
5[c]		92%	12		(78%)	18[j]		27% (25%) + 28%
6[d]		14%	13[h]		54% (55%)	19[k]		42%
7[e]		71% (68%)						

[a]Reaction conditions: Substrate (0.3 mmol), NH_3 (4 atm), Pd@Mg(OH)$_2$ (Pd: 5 mol %), solvent (DMA: 2 mL), 190 °C, 2 h. All reactions were conducted in a 40 mL pressure tube. Yields were determined by GC analysis using n-hexadecane as an internal standard. Isolated yields are shown in parentheses. [b]1 h. [c]6 h. [d]48 h. [e]3 h. [f]8 h. [g]50 °C, 1 h, followed by 190 °C, 3 h. [h]The isolated yield was shown after the subtraction of the amounts of residual solvents calculated from ^{1}H NMR. [i]1.5 h. [j]50 °C, 1 h, followed by 190 °C, 2 h. [k]50 °C, 0.5 h, followed by 190 °C, 1 h.

Chemical), Al$_2$O$_3$ (BET surface area: 160 m^2 g^{-1} after calcination at 600 °C for 3 h, KHS-24, Sumitomo Chemical), CeO$_2$ (BET surface area: 92 m^2 g^{-1}, JRC-CEO-5, Daiichi Kigenso Kagaku Kogyo), Mg$_6$Al$_2$(OH)$_{16}$CO$_3$·4H$_2$O (LDH, BET surface area: 47 m^2 g^{-1}, Tomita Pharmaceutical Co., Ltd.), ZrO$_2$ (BET surface area: 100.5 m^2 g^{-1}, JRC-ZRO-6, Catalysis Society of Japan), TiO$_2$ (BET surface area: 316 m^2 g^{-1}, ST-01, Ishihara Sangyo Kaisya), Pd/C (lot. no. 217-183621, N.E. CHEMCAT), Pt/C (lot. no. C-4634, Johnson Matthey), and Ru/C (lot. no. 417-020160, N.E. CHEMCAT) were commercially available. Solvents, substrates, and metal sources were obtained from Tokyo Chemical Industry, Sigma-Aldrich, Kanto Chemical, FUJIFILM Wako Pure Chemical, Nacalai Tesque, Kojima Chemicals, or Combi-Blocks (reagent grade).

Preparation of Catalysts

An Mg(OH)$_2$-supported Pd catalyst with the deposition of Mg(OH)$_2$ on the surface of Pd nanoparticles (Pd@Mg(OH)$_2$) was prepared as follows. First, MgO (2.0 g) was added to a 60 mL aqueous solution of PdCl$_2$ (12.5 mM) and KCl (2 equiv with respect to PdCl$_2$). After stirring vigorously for 15 min at room temperature, the pH of the solution became 10.5. The resulting slurry was further stirred at room temperature for 24 h. The solid was then filtered off, washed with water (3 L), and dried in vacuo overnight to afford the hydroxide precursor (brownish yellow powder). The hydroxide precursor was then dispersed in 50 mL of water for 30 min and reduced by NaBH$_4$ (75 mg). The resulting slurry was further stirred vigorously at room temperature for 2 h. The solid was again filtered off, washed with water (2 L), and dried in vacuo overnight to afford the Pd@Mg(OH)$_2$ catalyst (shallow gray powder, Pd: 0.26 mmol g^{-1}) (Figure S1a).

An Mg(OH)$_2$-supported Pd catalyst (Pd/Mg(OH)$_2$) was prepared as follows. First, MgO (2.0 g) was added to a beaker with 60 mL water. After stirring vigorously for 24 h at room temperature, the solid was then filtered off, washed with water (200 mL), and dried in vacuo

overnight to afford Mg(OH)$_2$ (white powder: 2.8 g). Then, Mg(OH)$_2$ (2.8 g) was added to a 60 mL aqueous solution of PdCl$_2$ (12.5 mM) and KCl (2 equiv with respect to PdCl$_2$). After stirring vigorously for 15 min at room temperature, the pH of the solution was adjusted from 9.5 to 10.5 using an aqueous solution of NaOH (1 M). The resulting slurry was further stirred at room temperature for 24 h. The solid was then filtered off, washed with water (3 L), and dried in vacuo overnight to afford the hydroxide precursor (brownish yellow powder). The hydroxide precursor was then dispersed in 50 mL of water for 30 min and reduced by NaBH$_4$ (75 mg). The resulting slurry was further stirred vigorously at room temperature for 2 h. The solid was again filtered off, washed with water (2 L), and dried in vacuo overnight to afford the Pd/Mg(OH)$_2$ catalyst (deep gray-black powder, Pd: 0.26 mmol g^{-1}) (Figure S1b).

An HAP-supported Pd catalyst (Pd/HAP) was prepared as follows. First, HAP (2.0 g) was added to a 60 mL of aqueous solution of PdCl$_2$ (8.3 mM) and KCl (2 equiv with respect to PdCl$_2$). After stirring vigorously for 15 min at room temperature, 1 M NaOH aq. was dropwise added to adjust the pH of the solution to 10.5. The resulting slurry was further stirred at room temperature for 24 h. The solid was then filtered off, washed with water (3 L), and dried in vacuo overnight to afford the hydroxide precursor (brownish yellow powder). The hydroxide precursor was then dispersed in 50 mL of water and reduced by NaBH$_4$ (75 mg). The resulting slurry was further stirred vigorously at room temperature for 2 h. The solid was again filtered off, washed with water (2 L), and dried in vacuo overnight to afford the Pd/HAP catalyst (black-gray powder, Pd: 0.23 mmol g^{-1}). Other supported Pd catalysts such as Pd/Al$_2$O$_3$ (Pd: 0.24 mmol g^{-1}), Pd/CeO$_2$ (Pd: 0.24 mmol g^{-1}), Pd/LDH (Pd: 0.25 mmol g^{-1}), Pd/ZrO$_2$ (Pd: 0.22 mmol g^{-1}), and Pd/TiO$_2$ (Pd: 0.21 mmol g^{-1}) were prepared by the similar methods. The supported Pd amounts were determined by ICP-AES analysis and are summarized in Table S8.

■ ASSOCIATED CONTENT

● SI Supporting Information

The Supporting Information is available free of charge at https://pubs.acs.org/doi/10.1021/jacsau.3c00049.

> Experimental details, additional experimental results, and spectral data of compounds (PDF)

■ AUTHOR INFORMATION

Corresponding Authors

Takafumi Yatabe − *Department of Applied Chemistry, School of Engineering, The University of Tokyo, Tokyo 113-8656, Japan; Precursory Research for Embryonic Science and Technology (PRESTO), Japan Science and Technology Agency (JST), Kawaguchi, Saitama 332-0012, Japan;* ● orcid.org/0000-0001-5504-4762; Email: yatabe@appchem.t.u-tokyo.ac.jp

Kazuya Yamaguchi − *Department of Applied Chemistry, School of Engineering, The University of Tokyo, Tokyo 113-8656, Japan;* ● orcid.org/0000-0002-7661-4936; Email: kyama@appchem.t.u-tokyo.ac.jp; Fax: +81-3-5841-7220

Authors

Hui Li − *Department of Applied Chemistry, School of Engineering, The University of Tokyo, Tokyo 113-8656, Japan*

Satoshi Takayama − *Department of Applied Chemistry, School of Engineering, The University of Tokyo, Tokyo 113-8656, Japan*

Complete contact information is available at:
https://pubs.acs.org/10.1021/jacsau.3c00049

Notes

The authors declare no competing financial interest.

■ ACKNOWLEDGMENTS

■ REFERENCES

(1) (a) Vogt, P. F.; Gerulis, J. J. *Amines, Aromatic: Ullmann's Encyclopedia of Industrial Chemistry*; Wiley-VCH: Weinheim, 2012; Vol. 2, pp 699−718. (b) Amini, B.; Lowenkron, S. *Aniline and its Derivatives: Kirk-Othmer Encyclopedia of Chemical Technology*; Wiley: Hoboken, 2003; Vol. 2, pp 783−809.

(2) Downing, R. S.; Kunkeler, P. J.; van Bekkum, H. Catalytic Syntheses of Aromatic Amines. *Catal. Today* **1997**, *37*, 121−136.

(3) (a) Fan, M.; Zhou, W.; Jiang, Y.; Ma, D. Assembly of Primary (Hetero)Arylamines via CuI/Oxalic Diamide-Catalyzed Coupling of Aryl Chlorides and Ammonia. *Org. Lett.* **2015**, *17*, 5934−5937. (b) Jiang, L.; Lu, X.; Zhang, H.; Jiang, Y.; Ma, D. CuI/4-Hydro-l-proline as a More Effective Catalytic System for Coupling of Aryl Bromides with *N*-Boc Hydrazine and Aqueous Ammonia. *J. Org. Chem.* **2009**, *74*, 4542−4546. (c) Xu, H.-J.; Liang, Y.-F.; Cai, Z.-Y.; Qi, H.-X.; Yang, C.-Y.; Feng, Y.-S. CuI-Nanoparticles-Catalyzed Selective Synthesis of Phenols, Anilines, and Thiophenols from Aryl Halides in Aqueous Solution. *J. Org. Chem.* **2011**, *76*, 2296−2300. (d) Cheung, C. W.; Surry, D. S.; Buchwald, S. L. Mild and Highly Selective Palladium-Catalyzed Monoarylation of Ammonia Enabled by the Use of Bulky Biarylphosphine Ligands and Palladacycle Precatalysts. *Org. Lett.* **2013**, *15*, 3734−3737. (e) Shen, Q.; Hartwig, J. F. Palladium-Catalyzed Coupling of Ammonia and Lithium Amide with Aryl Halides. *J. Am. Chem. Soc.* **2006**, *37*, 10028−10029. (f) Surry, D. S.; Buchwald, S. L. Selective Palladium-Catalyzed Arylation of Ammonia: Synthesis of Anilines as Well as Symmetrical and Unsymmetrical Di- and Triarylamines. *J. Am. Chem. Soc.* **2007**, *129*, 10354−10355. (g) Vo, G. D.; Hartwig, J. F. Palladium-Catalyzed Coupling of Ammonia with Aryl Chlorides, Bromides, Iodides, and Sulfonates: A General Method for the Preparation of Primary Arylamines. *J. Am. Chem. Soc.* **2009**, *131*, 11049−11061. (h) Kim, J.; Chang, S. Ammonium Salts as an Inexpensive and Convenient Nitrogen Source in the Cu-Catalyzed Amination of Aryl Halides at Room Temperature. *Chem. Commun.* **2008**, *26*, 3052−3054. (i) Rao, H.; Fu, H.; Jiang, Y.; Zhao, Y. Easy Copper-Catalyzed Synthesis of Primary Aromatic Amines by Couplings Aromatic Boronic Acids with Aqueous Ammonia at Room Temperature. *Angew. Chem., Int. Ed.* **2009**, *48*, 1114−1116. (j) Ruiz-Castillo, P.; Buchwald, S. L. Applications of Palladium-Catalyzed C−N Cross-Coupling Reactions. *Chem. Rev.* **2016**, *116*, 12564−12649. (k) Schranck, J.; Tlili, A. Transition-Metal-Catalyzed Monoarylation of Ammonia. *ACS Catal.* **2018**, *8*, 405−418.

(4) (a) Cuypers, T.; Tomkins, P.; De Vos, D. E. Direct Liquid-Phase Phenol-to-Aniline Amination Using Pd/C. *Catal. Sci. Technol.* **2018**, *8*, 2519−2523. (b) Qiu, Z.; Lv, L.; Li, J.; Li, C.-C.; Li, C.-J. Direct Conversion of Phenols into Primary Anilines with Hydrazine Catalyzed by Palladium. *Chem. Sci.* **2019**, *10*, 4775−4781. (c) Qiu, Z.; Zeng, H.; Li, C.-J. Coupling without Coupling Reactions: En Route to Developing Phenols as Sustainable Coupling Partners via Dearomatization−Rearomatization Processes. *Acc. Chem. Res.* **2020**, *53*, 2395−2413. (d) Liu, X.; Chen, W.; Zou, J.; Ye, L.; Yuan, Y. Liquid-Phase Amination of Phenol to Aniline over the Pd/MgO Catalyst without External Hydrogen Addition. *ACS Sustainable Chem. Eng.* **2022**, *10*, 6988−6998.

(5) Recently, Shi and coworkers reported Rh-catalyzed amination of phenols to arylamines via keto−enol tautomerization of phenols without requiring any reductants, although this system was not applied to primary aniline synthesis. See: Chen, K.; Kang, Q.-K.; Li, Y.; Wu, W. Q.; Zhu, H.; Shi, H. Catalytic Amination of Phenols with Amines. *J. Am. Chem. Soc.* **2022**, *144*, 1144−1151.

(6) (a) Romero, N. A.; Margrey, K. A.; Tay, N. E.; Nicewicz, D. A. Site-Selective Arene C−H Amination via Photoredox Catalysis. *Science* **2015**, *349*, 1326−1330. (b) Zheng, Y.-W.; Chen, B.; Ye, P.; Feng, K.; Wang, W.; Meng, Q.-Y.; Wu, L.-Z.; Tung, C.-H. Photocatalytic Hydrogen-Evolution Cross-Couplings: Benzene C−H Amination and Hydroxylation. *J. Am. Chem. Soc.* **2016**, *138*, 10080−10083. (c) Kim, H.; Heo, J.; Kim, J.; Baik, M.-H.; Chang, S. Copper-Mediated Amination of Aryl C−H Bonds with the Direct Use of Aqueous Ammonia via a Disproportionation Pathway. *J. Am. Chem. Soc.* **2018**, *140*, 14350−14356.

(7) (a) Izawa, Y.; Pun, D.; Stahl, S. S. Palladium-Catalyzed Aerobic Dehydrogenation of Substituted Cyclohexanones to Phenols. *Science* **2011**, *333*, 209−213. (b) Girard, S. A.; Huang, H.; Zhou, F.; Deng, G.-J.; Li, C.-J. Catalytic Dehydrogenative Aromatization: an Alternative Route to Functionalized Arenes. *Org. Chem. Front.* **2015**, *2*, 279−287. (c) Iosub, A. V.; Stahl, S. S. Palladium-Catalyzed Aerobic Dehydrogenation of Cyclic Hydrocarbons for the Synthesis

of Substituted Aromatics and Other Unsaturated Products. *ACS Catal.* **2016**, *6*, 8201−8213. (d) Liu, X.; Chen, J.; Ma, T. Catalytic Dehydrogenative Aromatization of Cyclohexanones and Cyclohexenones. *Org. Biomol. Chem.* **2018**, *16*, 8662−8676. (e) Girard, S. A.; Hu, X.; Knauber, T.; Zhou, F.; Simon, M.-O.; Deng, G.-J.; Li, C.-J. Pd-Catalyzed Synthesis of Aryl Amines via Oxidative Aromatization of Cyclic Ketones and Amines with Molecular Oxygen. *Org. Lett.* **2012**, *14*, 5606−5609. (f) Hajra, A.; Wei, Y.; Yoshikai, N. Palladium-Catalyzed Aerobic Dehydrogenative Aromatization of Cyclohexanone Imines to Arylamines. *Org. Lett.* **2012**, *14*, 5488−5491. (g) Sutter, M.; Duclos, M.-C.; Guicheret, B.; Raoul, Y.; Métay, E.; Lemaire, M. Straightforward Solvent-Free Heterogeneous Palladium-Catalyzed Synthesis of Arylamines from Nonaromatic Substrates by Dehydrogenative Alkylation. *ACS Sustainable Chem. Eng.* **2013**, *1*, 1463−1473. (h) Barros, M. T.; Dey, S. S.; Maycock, C. D.; Rodrigues, P. Metal-Free Direct Amination/Aromatization of 2-Cyclohexenones to Iodo-*N*-Arylanilines and *N*-Arylanilines Promoted by Iodine. *Chem. Commun.* **2012**, *48*, 10901−10903. (i) Zhao, J.; Huang, H.; Wu, W.; Chen, H.; Jiang, H. Metal-Free Synthesis of 2-Aminobenzothiazoles via Aerobic Oxidative Cyclization/Dehydrogenation of Cyclohexanones and Thioureas. *Org. Lett.* **2013**, *15*, 2604−2607. (j) Xie, Y.; Liu, S.; Liu, Y.; Wen, Y.; Deng, G.-J. Palladium-Catalyzed One-Pot Diarylamine Formation from Nitroarenes and Cyclohexanones. *Org. Lett.* **2012**, *14*, 1692−1695.

(8) (a) Koizumi, Y.; Jin, X.; Yatabe, T.; Miyazaki, R.; Hasegawa, J.; Nozaki, K.; Mizuno, N.; Yamaguchi, K. Selective Synthesis of Primary Anilines from NH₃ and Cyclohexanones by Utilizing Preferential Adsorption of Styrene on the Pd Nanoparticle Surface. *Angew. Chem., Int. Ed.* **2019**, *58*, 10893−10897. (b) Jin, X.; Koizumi, Y.; Yamaguchi, K.; Nozaki, K.; Mizuno, N. Selective Synthesis of Primary Anilines from Cyclohexanone Oximes by the Concerted Catalysis of a Mg−Al Layered Double Hydroxide Supported Pd Catalyst. *J. Am. Chem. Soc.* **2017**, *139*, 13821−13829. (c) Lin, W.-C.; Yatabe, T.; Yamaguchi, K. Selective Primary Aniline Synthesis through Supported Pd-Catalyzed Acceptorless Dehydrogenative Aromatization by Utilizing Hydrazine. *Chem. Commun.* **2021**, *57*, 6530−6533.

(9) U Dighe, S.; Juliá, F.; Luridiana, A.; Douglas, J. J.; Leonori, D. A. A photochemical dehydrogenative strategy for aniline synthesis. *Nature* **2020**, *584*, 75−81.

(10) (a) Jin, X.; Taniguchi, K.; Yamaguchi, K.; Mizuno, N. Au−Pd Alloy Nanoparticles Supported on Layered Double Hydroxide for Heterogeneously Catalyzed Aerobic Oxidative Dehydrogenation of Cyclohexanols and Cyclohexanones to Phenols. *Chem. Sci.* **2016**, *7*, 5371−5383. (b) Jin, X.; Taniguchi, K.; Yamaguchi, K.; Nozaki, K.; Mizuno, N. A Ni−Mg−Al layered triple hydroxide-supported Pd catalyst for heterogeneous acceptorless dehydrogenative aromatization. *Chem. Commun.* **2017**, *53*, 5267−5270. (c) Taniguchi, K.; Jin, X.; Yamaguchi, K.; Mizuno, N. Supported Gold−Palladium Alloy Nanoparticle Catalyzed Tandem Oxidation Routes to *N*-Substituted Anilines from Non-Aromatic Compounds. *Chem. Commun.* **2015**, *51*, 14969−14972. (d) Taniguchi, K.; Jin, X.; Yamaguchi, K.; Mizuno, N. Facile Access to *N*-Substituted Anilines via Dehydrogenative Aromatization Catalysis over Supported Gold−Palladium Bimetallic Nanoparticles. *Catal. Sci. Technol.* **2016**, *6*, 3929−3937. (e) Taniguchi, K.; Jin, X.; Yamaguchi, K.; Nozaki, K.; Mizuno, N. Versatile Routes for Synthesis of Diarylamines through Acceptorless Dehydrogenative Aromatization Catalysis over Supported Gold−Palladium Bimetallic Nanoparticles. *Chem. Sci.* **2017**, *8*, 2131−2142. (f) Koizumi, Y.; Taniguchi, K.; Jin, X.; Yamaguchi, K.; Nozaki, K.; Mizuno, N. Formal Arylation of NH₃ to Produce Diphenylamines over Supported Pd Catalysts. *Chem. Commun.* **2017**, *53*, 10827−10830. (g) Oyama, T.; Yatabe, T.; Jin, X.; Mizuno, N.; Yamaguchi, K. Heterogeneously Palladium-catalyzed Acceptorless Dehydrogenative Aromatization of Cyclic Amines. *Chem. Lett.* **2019**, *48*, 517−520. (h) Takayama, S.; Yatabe, T.; Koizumi, Y.; Jin, X.; Nozaki, K.; Mizuno, N.; Yamaguchi, K. Synthesis of Unsymmetrically Substituted Triarylamines via Acceptorless Dehydrogenative Aromatization Using a Pd/C and *p*-Toluenesulfonic Acid Hybrid Relay Catalyst. *Chem. Sci.* **2020**, *11*, 4074−4084.

(11) Some patents reported the synthesis of primary anilines from NH₃ and cyclohexanones, which were carried out in gas phases, required quite high reaction temperatures/pressures, possessed limited substrate scopes, and/or caused the low selectivity to primary anilines, for examples, see: (a) Wilder, G. R.; Verth, J. E. V. Manufacture of Aromatic Amines from Alicyclic Ketones. U.S. Patent 3,219,704 A, 1965. (b) Solomon, J. M.; Bluestein, B. R. Process for Preparing Aniline. U.S. Patent 3,553,268 A, 1971. (c) Goetz, N.; Hupfer, L.; Hoffmann, W.; Baumann, M. Preparation of Primary Aromatic Amines from Cyclic Alcohols and/or Ketones. U.S. Patent 4,355,180 A, 1982. (d) Haese, F.; Wulff-Doring, J.; Kohler, U.; Gaa, P.; Pape, F.-F.; Melder, J.-P.; Julius, M. Process for Continuous Preparation of a Primary Aromatic Amine. U.S. Patent 20,090,076,306 A1, 2009.

(12) (a) Niu, F.; Xie, S.; Bahri, M.; Ersen, O.; Yan, Z.; Kusema, B. T.; Pera-Titus, M.; Khodakov, A. Y.; Ordomsky, V. V. Catalyst Deactivation for Enhancement of Selectivity in Alcohols Amination to Primary Amines. *ACS Catal.* **2019**, *9*, 5986−5997. (b) Wu, D.; Wang, Q.; Safonova, O. V.; Peron, D. V.; Zhou, W.; Yan, Z.; Marinova, M.; Khodakov, A. Y.; Ordomsky, V. V. Lignin Compounds to Monoaromatics: Selective Cleavage of C−O Bonds over a Brominated Ruthenium Catalyst. *Angew. Chem., Int. Ed.* **2021**, *60*, 12513−12523. (c) Mitsudome, T.; Yamamoto, M.; Maeno, Z.; Mizugaki, T.; Jitsukawa, K.; Kaneda, K. One-step Synthesis of Core-Gold/Shell-Ceria Nanomaterial and Its Catalysis for Highly Selective Semihydrogenation of Alkynes. *J. Am. Chem. Soc.* **2015**, *137*, 13452−13455.

(13) The catalytic activity of Pd@Mg(OH)₂ for the dehydrogenative aromatization of **3a** to **2a** was considerably lower than that of Pd/Mg(OH)₂, which also suggested the deposition of Mg(OH)₂ on the Pd nanoparticles in Pd@Mg(OH)₂.

(14) When the dehydrogenative aromatization reactions of **1a** to **4a** were conducted at 190 °C for 5 min in the presence of Pd@Mg(OH)₂ or Pd/Mg(OH)₂, the same tendency was observed; the reaction hardly proceeded in the presence of Pd@Mg(OH)₂, whereas Pd/Mg(OH)₂ gave **4a** in a high yield (Scheme S4).

(15) (a) Delbecq, F.; Sautet, P. Adsorption of Aldehydes and Ketones on Platinum and Palladium: Influence of Steps, Open Faces and Metal Nature. *Surf. Sci.* **1993**, *295*, 353−373. (b) Carneiro, J. W. d. M.; Cruz, M. T. d. M. Density Functional Theory Study of the Adsorption of Formaldehyde on Pd₄ and on Pd₄/γ-Al₂O₃ Clusters. *J. Phys. Chem. A* **2008**, *112*, 8929−8937. (c) McManus, J. R.; Salciccioli, M.; Yu, W.; Vlachos, D. G.; Chen, J. G.; Vohs, J. M. Correlating the Surface Chemistry of C₂ and C₃ Aldoses with a C₆ Sugar: Reaction of Glucose, Glyceraldehyde, and Glycolaldehyde on Pd(111). *J. Phys. Chem. C* **2012**, *116*, 18891−18898.

(16) Schröder, C.; Schmidt, M. C.; Haugg, P. A.; Baumann, A.-K.; Smyczek, J.; Schauermann, S. Understanding Ligand-Directed Heterogeneous Catalysis: When the Dynamically Changing Nature of the Ligand Layer Controls the Hydrogenation Selectivity. *Angew. Chem., Int. Ed.* **2021**, *60*, 16349−16354.

(17) The differences of adsorption modes are typically investigated on the Pd(111) plane,[15,16] and the lattice spacings identical to the (111) plane of Pd (d_{111} = ∼0.23 nm) were observed in the HAADF-STEM images of Pd/Mg(OH)₂ (Figure S4) although clear planes of Pd nanoparticles were hardly observed in Pd@Mg(OH)₂ probably due to the presence of Mg(OH)₂ on the Pd surface (Figure S3).

(18) A similar preferential adsorption inhibition of secondary imines was reported for a cobalt catalyst with carbon deposition.[12a]

(19) Considering that α,β-unsaturated imines were not detected during the reactions, primary aniline formation from α,β-unsaturated imines proceeded very quickly on Pd nanoparticle catalysts. One possible reason for the fast dehydrogenation is that α,β-unsaturated imines are successively dehydrogenated before desorption from the catalyst. The other possible reason is that the fast disproportionation of α,β-unsaturated imines to primary anilines and cyclohexanimines occurs on Pd nanoparticles like previously reported phenol formation via Pd nanoparticles-catalyzed disproportionation of cyclohexenones.[10a,b]